Bidentate chemisorption of acetic acid on a Si(001)-(2×1) surface: Experimental and theoretical investigations

Masaru Shimomura,* Takenori K. Kawaguchi, Yasuo Fukuda, and Kenji Murakami
Research Institute of Electronics, Shizuoka University, 3-5-1 Johoku, Naka-ku, Hamamatsu 432-8011, Japan

A. Z. AlZahrani and G. P. Srivastava
School of Physics, University of Exeter, Stocker Road, Exeter EX4 4QL, United Kingdom
(Received 25 March 2009; published 22 October 2009)

Adsorption of acetic acid on the Si(001)-(2×1) surface is studied by x-ray photoelectron spectroscopy (XPS), scanning-tunneling microscopy (STM), and *ab initio* calculations. We find that C 1*s* line of the acetic acid on the surface is composed of mainly methyl and adsorbed carboxyl groups. The filled-state STM images indicate that protrusions of the adsorbate are located on center of single Si dimer. The on-top configuration with a vertical Si-O-C(CH_3)-O-Si linkage to the Si dimer is supported by these XPS and STM results. The *ab initio* calculations show a plausible reaction pathway from the initial adsorption structure with O-H cleavage to the on-top configuration.

DOI: 10.1103/PhysRevB.80.165324 PACS number(s): 68.43.Mn, 68.35.Md, 68.37.Ef

I. INTRODUCTION

Numerous studies on reactions of organic molecules with Si surfaces have been performed to establish molecular- and bio-electronic devices based on the Si nanotechnology. Since carboxylic acid is an industrially and medicinally useful molecule, studies on its chemical reactivity on a Si surface will provide a fundamental knowledge for practical applications. In the past, adsorption structures of various carboxylic acids on the Si(001)-(2×1) surface have been studied and the O-H bond cleavage, which results in the R-COO-Si and H-Si adsorbates on the surface, has been reported.[1–7] Acetic acid is the simplest organic molecules containing the carboxyl group. While many studies have been reported on the adsorption of acetic acid on transition-metal surfaces, there are relatively fewer studies of its adsorption on semiconductor surfaces. First-principles calculations have also been performed to investigate reaction pathways of the adsorption of this molecule.[1,8] Carbone and Caminiti[8] found that the molecule can be initially adsorbed on the surface dissociatively, either via the O-H bond cleavage or via the C-H bond cleavage. Kim and Cho[1] on the other hand, reported that the molecule can be adsorbed either dissociatively through the O-H bond cleavage or in a [2+2] cycloaddition reaction (i.e., forming di-σ bonds between C=O moiety and the Si dimer). The work by Kim and Cho further suggested that the molecule is thermally desorbed from the [2+2] cycloaddition configuration at RT, leaving the dissociative configuration more likely. Their suggested dissociative adsorption model is the monodentate (MD) configuration shown in Fig. 1. Very recently, high-resolution photoelectron spectroscopy and near-edge x-ray absorption fine-structure (NEXAFS) study also concluded that the adsorption structure agrees with the MD configuration because of the following reasons: (1) Si-O and Si-H components exist in the Si 2*p* core-level spectrum, (2) C 1*s* and O 1*s* core-level spectra of the acetic-acid-adsorbed surface are in agreement with those of the acetic-acid-adsorbed Ge(001) surface,[9] and (3) existence of a π^* orbital for the C=O bond is found in NEXAFS. However, the recent scanning-tunneling microscopy (STM) study of acetic-acid adsorption on the Ge(001)-(2×1) surface[10,11] shows the possibility of the bidentate end-bridged (EB) and bidentate on-top (OT) configurations at the substrate temperature of 300 and 400 K, respectively.

In this study, we report a chemisorption structure of acetic acid on the Si(001)-(2×1) surface studied by STM, x-ray photoelectron spectroscopy (XPS), and *ab initio* calculations based on density-functional theory (DFT). A plausible adsorbate configuration is presented and the surface reaction of acetic acid on the surface is discussed in terms of the total energy.

II. EXPERIMENTAL AND THEORETICAL PROCEDURES

A Si(001) sample was degreased by acetone and ethanol and subsequently rinsed by distilled water. After the sample

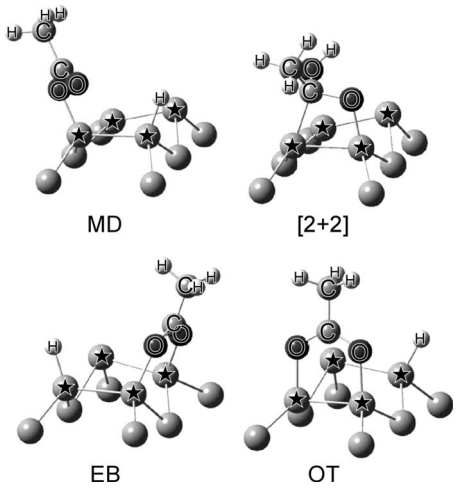

FIG. 1. Schematic of the possible configurations of acetic acid on the Si(001)-(2×1) surface. MD: the monodentate structure, [2+2]: the [2+2] cycloaddition structure, EB: the end-bridged bidentate structure, OT: the on-top bidentate structure. The surface dimer atoms are marked with a star.

was chemically etched by an Hartree-Fock solution, it was installed into an ultra-high vacuum (UHV) chamber. The sample was cleaned by a few cycles of flashing at 1250 °C. After the flashing, clear (2×1) low-energy electron diffraction patterns with low background were observed. The sample was kept over 15 min under UHV condition for heat dissipation. The temperature was measured by a pyrometer that is detectable over 200 °C. It took ~5 min to become <200 °C after flashing. Then, leaving the sample in UHV for additional 10 min provides the substrate temperature in between 30 and 80 °C. After this cooling-down procedure, it was estimated by XPS that about 5% of surface dimers were contaminated. This surface was then exposed to acetic-acid gas. The acetic-acid gas was ejected to the chamber through a leak valve with a leading nozzle that is spaced 20 mm from the sample. Here, the exposure (in Langmuir, L) was simply calculated from the pressure measured by an ion gauge distanced 200 mm away from end of the nozzle. The real exposure at the surface would be higher than the noted value. The experiments were performed in the UHV systems with a base pressure of 10^{-8} Pa. The STM facility was a commercial unit from JEOL (model JSTM-4500XT). XPS measurements were performed using ESCA-LAB Mk II (VG) with Mg $K\alpha$ excitation source (1253.6 eV).

For theoretical studies, we have modeled the system by using a repeated supercell structure. Each unit cell is based on a (2×2) reconstructed Si(001) surface mesh and contains six silicon layers, acetic acid, and a vacuum region equivalent to about five substrate layers in thickness (~20 Å). The back surface of the slab was saturated with two pseudohydrogen atoms per Si atom. The total-energy calculations presented in this paper were performed in the framework of the DFT (Ref. 12) within the generalized-gradient approximation. The Perdew-Burke-Ernzerh exchange-correlation scheme[13] was considered to treat the electron-electron interactions. The electron-ion interactions were treated by using the ultrasoft pseudopotentials.[14] The single-particle Kohn-Sham[15] wave functions were expanded in the framework of a plane-wave basis set. Test calculations have shown that a kinetic-energy cutoff for the wave functions equal to 25 Ryd is sufficient to obtain well-converged results. Throughout the calculations we use the calculated Si equilibrium lattice constant of 5.42 Å. Self-consistent solutions of the Kohn-Sham equations were obtained by employing a $2\times2\times1$ **k**-points Monkhorst-Pack set[16] within the surface Brillouin zone. The Hellman-Feynman forces on ions were calculated and minimised to obtain the relaxed atomic geometry. The equilibrium atomic positions were determined by relaxing all atoms in the unit cell except the two bottom Si layers which were kept frozen into their bulk positions.

III. RESULTS AND DISCUSSION

Figures 2(a) and 2(b) show C 1*s* XPS core-level spectra taken at the exposure of 0–25 L and the curve-fitting result of the spectrum at 25 L, respectively. Intensity of C 1*s* is saturated at the exposure of 2.5 L. The saturation coverage of the acetic-acid molecule is estimated to ~0.25 monolayer (ML). Because one molecule occupies one dimer, i.e., two surface

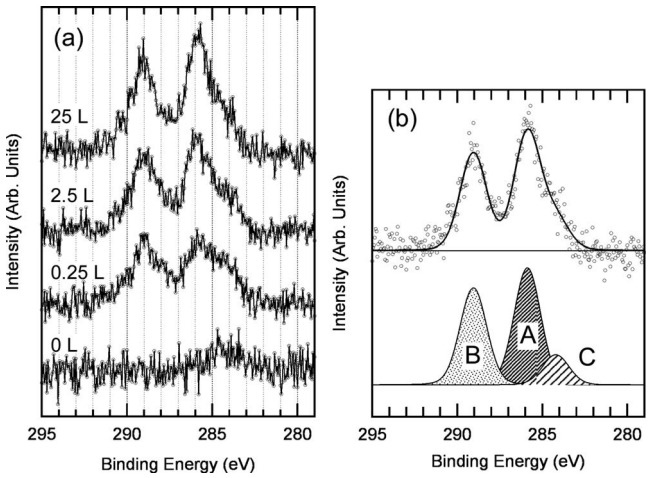

FIG. 2. (a) C 1*s* core-level spectra taken after the acetic-acid exposure of 0–25 L. The excitation energy is 1253.6 eV (Mg $K\alpha$ line). Detection angle is fixed at 75° off from the surface normal. (b) Curve fitting results of the spectrum at the exposure of 25 L. Width of the Lorentzian function was fixed to 0.2 eV. Width of the Gaussian function was 1.7 eV for all components. Peak positions are 285.9, 289.1, and 284.2 eV for A, B, and C, respectively.

Si atoms, ~50% of surface dimers are covered with acetic-acid species. The C 1*s* spectrum of the saturated surface can be fitted by three components: two main peaks at 285.9 eV (labeled "A"), 289.1 eV (labeled "B"), and a minor component at 284.2 eV (labeled "C"). The minor peak C is assigned to contamination since it is observed prior to the exposure [Fig. 2(a), 0 L]. The chemical shift to lower binding energy indicates that the contamination C could be related to SiC or a $Si_{1-x}C_x$ alloy structure.[17] The energy difference between the peaks A and B is 3.2 eV and it is in good agreement with the values for acetic acid adsorbed on the Si(001)-(2×1) and Ge(001)-(2×1) surfaces.[9,18] Following the literature, the peaks A and B can be assigned to the methyl and carboxyl carbons, respectively. There is no drastic change in the structure for coverage from 0.25 to 25 L, as the energy difference between the peaks remains constant. The energy difference of the two carbons of a free acetic-acid molecule is 4.5 eV.[19] Compared with this energy difference of the molecule, the energy difference for the adsorbate of 3.2 eV indicates a smaller oxidation state of the adsorbed carboxyl carbon atom. It is consistent with the bidentate EB and OT configurations. The core-level spectrum of O 1*s* can be fitted by one broad Gaussian function as in Refs. 9 and 18. However, it is difficult to estimate the structure from the O 1*s* spectrum because of lack of the energy resolution of the XPS instrument.

Panels (a) and (b) in Fig. 3 show filled-state STM images taken after exposure of 0.01 and 0.1 L, respectively. In Fig. 3(a), bright protrusions, indicated by arrows, can be observed. In Fig. 3(b), the number of the protrusions has increased, thus confirming that they correspond to the acetic-acid adsorbate. It should be noted that the adsorbates tend not to adsorb on a neighboring dimer capped with another adsorbate locally forming $p(2\times2)$ or $c(4\times2)$. It is in agreement with the saturation coverage of 0.5 ML estimated by XPS. To determine the precise position of the adsorbate, a

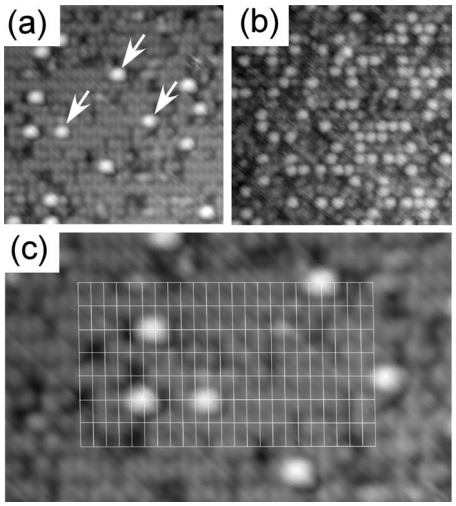

FIG. 3. Filled state STM images of acetic-acid-adsorbed Si(001)-(2×1) surface after the exposure of (a) 0.01 L and (b) 0.1 L with image size of 7.3 nm×7.3 nm. Sample bias and tunneling current are −3.5 V and 0.3 nA, respectively. (c) Magnified image of (a) with guided lines located on dimer bonds (vertical lines) and center of dimer rows (horizontal lines). Schematics of the Si dimer are also superimposed.

part of Fig. 3(a) is magnified as Fig. 3(c) with guided lines located on dimer bonds (vertical lines) and center of dimer rows (horizontal lines). Each protrusion is located on a Si dimer. Thus, the STM result shows that the acetic acid is adsorbed in the OT configuration. This view is also supported by the previous STM study,[11] in which filled-state images of the OT configuration of an adsorbed acetic acid on Ge(001)-(2×1) appeared as a round protrusion similar to that in Fig. 3. A number of asymmetric dimers and defects (black in intensity) are observed near the adsorbates. A dissociated hydrogen atom would induce static buckling of dimers and/or defects as well as adsorption of a water molecule from residual gas. In STM, a minute amount of off-centered protrusions that may be related to the EB or MD configurations were also observed. However the trivial percentage of such feature, less than 2–3 %, indicates that these protrusions are in a metastable structure. Theoretically predicted reaction pathway reveals the transient formation of the metastable structures.

In order to further establish support for the OT model we performed total-energy calculations for four plausible geometries: two monodentate structures (MD1 and MD2) and two bidentate structures (an end-bridge EB structure and the on-top OT structure). These are shown in Fig. 4. In the MD1 structure we consider dissociative molecular adsorption through the O-H bond cleavage. In this configuration, both the dissociated hydrogen atom and the fragmented acid are attached to the two Si atoms of a single Si dimer. In the MD2 structure the CH_3COO radical and the dissociated hydrogen are attached to two adjacent Si dimers. Following the suggestion from Refs. 10 and 11, in the EB configuration the CH_3COO radical is attached to the same component of two neighboring Si dimers and the dissociated hydrogen is attached to the other component of one of the two Si dimers. For the OT configuration the CH_3COO radical is chemisorbed to both components of one Si dimer and the dissociated hydrogen is attached to one component of the neighboring Si dimer.

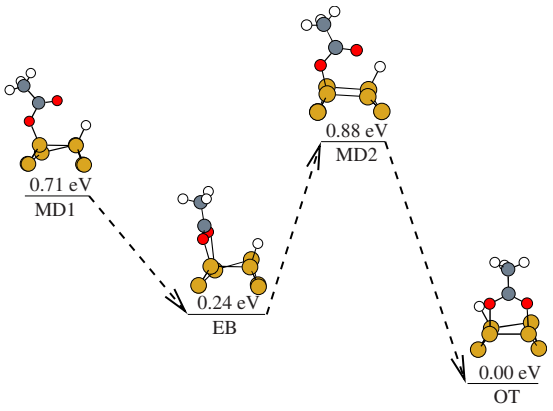

FIG. 4. (Color online) A plausible reaction pathway between the MD and OT configurations. The total energies are presented relative to that of the OT configuration. The radicals CH_3COO and H are attached to a single Si dimer in the MD1 configuration and to two neighboring Si dimmers in the MD2 configuration.

Our calculations suggest that OT is the lowest energy configuration. The total energy of MD1(MD2) is +0.88(0.71) eV relative to that of the relaxed OT configuration. An intercomparison of the total energies of the MD1 and MD2 configurations suggests that an energy saving of 0.17 eV can be achieved by the adsorption of the two fragments (CH_3COO and H) on a single Si-Si dimer rather than two adjacent Si dimers. This is achieved through a strain relieving mechanism: compared to MD1, the Si-Si dimer bond length and the Si-O bond length have increased, respectively, by 2.5% and 1.1% for the MD2 configuration.

Our calculations also suggest that upon full atomic relaxation the EB configuration loses its bidentate signature. From the resulting relaxed atomic geometry we found that one of the Si-O bond lengths (O atom attached to the bare Si-Si dimer) is much larger (approximately 2.0 Å) than the typical Si-O bond length (1.63 Å), leading the bond to break. In other words, it indicates that the formation of the chemical Si-O bond is not satisfied in this model. As indicated in Fig. 4, the total energy of the relaxed EB configuration is 0.24 eV higher than that for the OT configuration. In order to ensure a chemical bond formation between Si and O we also attempted a "constrained geometry" optimization: in this we fixed that O atom (in addition to the bottom Si layer in the supercell) and relaxed all other atoms. This resulted in both Si-O bond length to be nearly identical (1.86 Å) and in agreement with the Si-O bond length for the OT structure. However, the resulting total energy was much higher than the energy of the OT model, by approximately 1.12 eV. Thus, contrary to the suggestion on Ge,[10,11] we do not regard EB as a stable bidentate structure on Si. Thus OT is the dominant bidentate configuration. For the OT configuration, the Si-O bond length is comparable to the sum of the Si and O atomic radii. Furthermore, our calculations suggest that the two asymmetrical bond lengths between C and O in the free acetic molecule [viz., d(C=O)=1.21 Å and d(C-O)=1.36 Å] have become equal (1.285 Å) upon the molecular adsorption

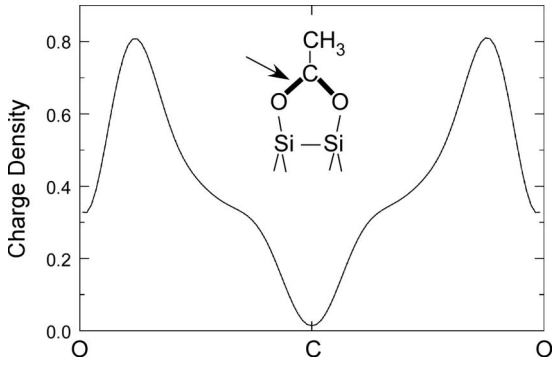

FIG. 5. Total charge-density plot for the OT configuration along the line including the C atom with the O atoms in the carboxyl group.

in the OT configuration. Our structural results for MD2 and OT are similar to those obtained by Carbone and Caminiti.[8]

The relaxed OT configuration forms a vertical pentagon Si-O-C-O-Si ring. In Fig. 5 we have plotted the total charge density along the lines joining the C atom with the two neighboring O atoms in the carboxyl group. Our calculations show that the C-O bond is partly covalent and partly ionic with a significant amount of its charge being transferred from C to O. We have employed a simple scheme to estimate the amount of charge transfer from C to O. In this scheme we have calculated the total charge density in a sphere around the C atom of radius equivalent to the distance between the C and O atoms. Using the same procedure we also determined the amount of charge around a single C atom placed in the unit cell that was used for the surface calculations. Using the numerical results from these two calculations, we find that approximately 94% of charge has been equally transferred from the C atom toward its neighboring O atoms. This result clearly indicates that the C atom of the carboxyl group is positively charged.

In order to provide support to the analysis of the experimental STM image in Fig. 3, we have theoretically simulated STM images of the surface with the OT configuration around the Si-Si dimer. The simulation of these STM images was performed using the Tersoff-Hamann method[20] in the constant-height mode. The tunneling current was derived from the local density of states close to the Fermi energy E_F. The panels (a) and (b) in Fig. 6 show the total charge density in the vertical plane passing through the molecule attached to the Si-Si dimer for the occupied and unoccupied states, respectively. The charge distribution in the occupied state shows that the Si-Si dimer bonding is intact and there is evidence of Si-O bonding. In the unoccupied state, as expected, the antibonding characteristics is evident. In panel (c) we show the filled-state STM image for a bias voltage of −3.5 eV. Different choices for the plotting plane (i.e., heights above the Si-Si dimer) were considered with similar overall image. The plotting plane in panel (c) passes through the carbon atom closer to oxygen. Significantly different values of local charge-density accumulation are seen on alternate Si-Si dimers along the dimer row. Much reduced brightness is seen at the alternate Si-Si dimers to which the molecular ion is attached. The brightness of the H-attached

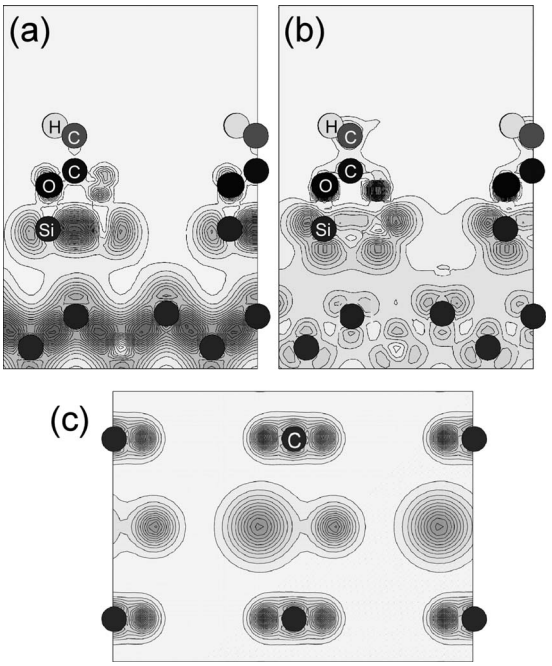

FIG. 6. Total charge-density plots in the vertical plane passing through the molecule attached to the Si-Si dimer: (a) occupied states and (b) unoccupied states. The simulated filled-state STM image in the constant-height mode passing through the carbon atom closer to the oxygen atom, with the bias of −3.5 eV, is shown in panel (c).

Si-Si dimers is asymmetric with larger protrusion on the bare component. The strongest and asymmetric brightness of the alternate Si-Si dimers is supportive of the experimental STM images in Fig. 3.

IV. CONCLUSIONS

In conclusion, we studied the adsorption of acetic acid on the Si(001)-(2×1) surface by XPS, STM, and DFT. The C 1*s* XPS core-level spectra can be fitted by mainly methyl and adsorbed carboxyl carbons with an energy difference of 3.2 eV. In filled-state STM images, individual protrusions of the adsorbate molecules are located on top of Si dimers. Thus, the OT configuration was supported by the XPS and STM results. The DFT calculations have shown a plausible reaction path between MD and OT configurations. The calculations have also detailed the equilibrium atomic geometry for OT. Furthermore, the theoretically simulated STM images are consistent with the experimental filled-state image and support the OT configuration for the adsorption of the acetic acid on the Si(001)-(2×1) surface.

ACKNOWLEDGMENTS

A. AlZahrani gratefully acknowledges financial support from King Abdulaziz University (KAU), Saudi Arabia. The calculations reported here were performed using the University of Exeter's SGI Altix ICE 8200 supercomputer. G.P.S. acknowledges visitors support from the CCP3 (UK).

*Corresponding author; rmshimo@ipc.shizuoka.ac.jp

[1] H.-J. Kim and J.-H. Cho, Phys. Rev. B **72**, 195305 (2005).
[2] H. Ikeura-Sekiguchi and T. Sekiguchi, Surf. Sci. **433-435**, 549 (1999).
[3] X. Lu, Q. Zhang, and M. C. Lin, Phys. Chem. Chem. Phys. **3**, 2156 (2001).
[4] T. Bitzer, T. Alkunshalie, and N. V. Richardson, Surf. Sci. **368**, 202 (1996).
[5] T. Bitzer and N. V. Richardson, Surf. Sci. **427-428**, 369 (1999).
[6] A. Lopez, T. Bitzer, T. Heller, and N. V. Richardson, Surf. Sci. **480**, 65 (2001).
[7] H.-N. Hwang, J.-Y. Baik, K.-S. An, S.-S. Lee, Y.-S. Kim, C.-C. Hwang, and B.-S. Kim, J. Phys. Chem. B **108**, 8379 (2004).
[8] M. Carbone and R. Caminiti, Surf. Sci. **602**, 852 (2008).
[9] M. A. Filler, J. A. Van Deventer, A. J. Keung, and S. F. Bent, J. Am. Chem. Soc. **128**, 770 (2006).
[10] D. H. Kim, E. Hwang, S. Hong, and S. Kim, Surf. Sci. **600**, 3629 (2006).
[11] E. Hwang, D. H. Kim, Y. J. Hwang, A. Kim, S. Hong, and S. Kim, J. Phys. Chem. C **111**, 5941 (2007).
[12] P. Hohenberg and W. Kohn, Phys. Rev. **136**, B864 (1964).
[13] J. P. Perdew, K. Burke, and M. Ernzerhof, Phys. Rev. Lett. **77**, 3865 (1996).
[14] D. Vanderbilt, Phys. Rev. B **41**, 7892 (1990).
[15] W. Kohn and L. Sham, Phys. Rev. **140**, A1133 (1965).
[16] H. J. Monkhorst and J. D. Pack, Phys. Rev. B **13**, 5188 (1976).
[17] R. Kosugi, T. Abukawa, M. Shimomura, S. Sumitani, H.-W. Yeom, T. Hanano, K. Tono, S. Suzuki, S. Sato, T. Ohta, S. Kono, and Y. Takakuwa, J. Electron Spectrosc. Relat. Phenom. **101-103**, 239 (1999).
[18] H.-K. Lee, K. Ki-jeong, H. Jin-hee, T.-H. Kang, J. W. Chung, and Bongsoo Kim, Phys. Rev. B **77**, 115324 (2008).
[19] U. Gelius, P. F. Hedén, J. Hedman, B. J. Lindberg, R. Manne, R. Nordberg, C. Nordling, and K. Siegbahn, Phys. Scr. **2**, 70 (1970).
[20] J. Tersoff and D. R. Hamann, Phys. Rev. B **31**, 805 (1985).